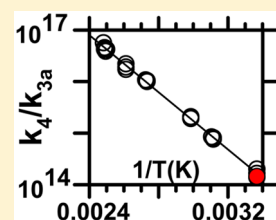


# Study of the Reaction Cl + Ethyl Formate at 700–950 Torr and 297 to 435 K: Product Distribution and the Kinetics of the Reaction $C_2H_5OC(=O) \rightarrow CO_2 + C_2H_5$

E. W. Kaiser\*

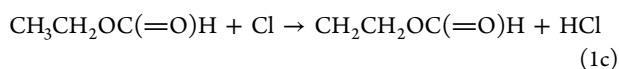
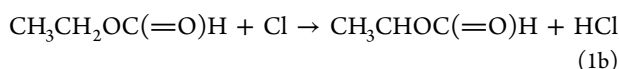
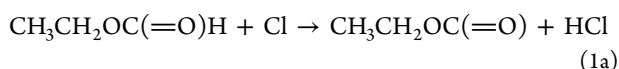
Department of Natural Sciences, University of Michigan-Dearborn, 4901 Evergreen Road, Dearborn, Michigan 48128, United States

**ABSTRACT:** The kinetics and mechanism of the reaction of atomic chlorine with ethyl formate [Cl + CH<sub>3</sub>CH<sub>2</sub>O(C=O)H, reaction 1] have been examined. These experiments were performed at pressures of 760–950 Torr and temperatures from 297 to 435 K. Reactants and products were quantified by gas chromatography–flame ionization detector (GC/FID) analysis. The initial mixture contained ethyl formate, Cl<sub>2</sub>, and N<sub>2</sub>. Cl atoms were generated by UV photolysis of this initial mixture at 360 nm, which dissociates Cl<sub>2</sub>. The rate constant of reaction 1 was measured at 297 K relative to that of the reaction Cl + C<sub>2</sub>H<sub>5</sub>Cl (reaction 2), yielding the rate constant ratio  $k_1/k_2 = 1.09 \pm 0.05$ . The final products formed from reaction 1 are ethyl chloroformate, 1-chloroethyl formate, and 2-chloroethyl formate. These products result from the reactions with Cl<sub>2</sub> of the three free radicals formed by H atom abstraction from ethylformate in reaction 1. Based on the molar yields of these three chlorinated products, the yields of the three radicals formed from reaction 1 at 297 K are (25 ± 3) mole percent of CH<sub>3</sub>CH<sub>2</sub>O(C=O); (67 ± 5) mole percent of CH<sub>3</sub>CHO(C=O)H; and (8 ± 2) mole percent of CH<sub>2</sub>CH<sub>2</sub>O(C=O)H. A second phase of this experiment measured the rate constant of the decarboxylation of the ethoxy carbonyl radical [CH<sub>3</sub>CH<sub>2</sub>O(C=O) → CO<sub>2</sub> + C<sub>2</sub>H<sub>5</sub>, reaction 4] relative to the rate constant of its reaction with Cl<sub>2</sub> [CH<sub>3</sub>CH<sub>2</sub>O(C=O) + Cl<sub>2</sub> → CH<sub>3</sub>CH<sub>2</sub>O(C=O)Cl + Cl, reaction 3a]. Over the temperature range 297 to 404 K at 1 atm total pressure, this ratio can be expressed by  $k_4/k_{3a} = 10^{23.56 \pm 0.22} e^{-(12700 \pm 375)/RT}$  molecules cm<sup>-3</sup>. Estimating the value of  $k_{3a}$  (which has not been measured) based on similar reactions, the expression  $k_4 = 5.8 \times 10^{12} e^{-(12700)/RT} s^{-1}$  is obtained. The estimated error of this rate constant is ± a factor of 2 over the experimental temperature range. This rate expression is compared with recent ab initio calculations of the decarboxylation of the analogous methoxy carbonyl radical.



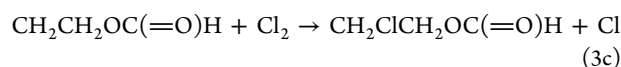
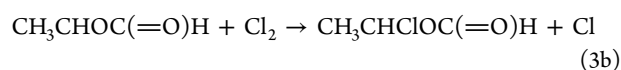
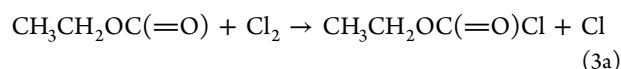
## 1. INTRODUCTION

In a recent publication,<sup>1</sup> the overall rate constant of the reaction of Cl with ethyl formate [Cl + CH<sub>3</sub>CH<sub>2</sub>O(C=O)H, reaction 1] was measured as a function of temperature relative to that of the reaction of Cl with C<sub>2</sub>H<sub>5</sub>Cl (reaction 2). The yield of each of the three abstraction product channels for reaction 1 was estimated using ab initio calculations in that publication. These calculations indicated that the major product channel was that represented by reaction 1b, which contributed 66.9% to the overall reaction rate constant at 298 K. Channel 1a contributed 33%, and channel 1c was predicted to contribute 0.1% to the total rate constant:



In the current experiments, the overall rate constant of reaction 1 is measured relative to that of reaction 2 at 297 K using the relative rate method. These experiments are performed in mixtures of ethyl formate, ethyl chloride, and

Cl<sub>2</sub> for comparison to the rate constant ratios  $k_1/k_2$  determined at ambient temperature using the same reference compound by Balaganesh et al.<sup>1</sup> and by Wallington et al.<sup>2</sup> In addition, the yields of the free radical product channels 1a–1c are determined experimentally from the yields of the chloride products (ethyl chloroformate, 1-chloroethyl formate, and 2-chloroethyl formate) formed by reactions 3a–3c.



Finally, the rate constant of reaction 4, the decomposition (decarboxylation) of the ethoxy carbonyl radical formed in reaction 1a [CH<sub>3</sub>CH<sub>2</sub>O(C=O)] to CO<sub>2</sub> and CH<sub>3</sub>CH<sub>2</sub>, is determined relative to that of its reaction with Cl<sub>2</sub> (reaction 3a) over the temperature range 297–404 K. The relative rate constant ratio,  $k_4/k_{3a}$  is obtained by measuring the molar yields

Received: March 16, 2016

Revised: April 16, 2016

of the ethyl chloride and ethyl chloroformate products formed by reactions 5 and 3a, respectively.



Gas-phase decarboxylation reactions of the type represented by reaction 4 are potentially important in the combustion of biodiesel fuels containing ester components.<sup>3</sup> Its methyl analogue ( $\text{CH}_3\text{OC}(=\text{O}) \rightarrow \text{CH}_3 + \text{CO}_2$ ) has been studied extensively in theoretical calculations as summarized by McCunn et al.,<sup>4</sup> Bell et al.<sup>5</sup> and Tan et al.<sup>6</sup> Although experimental rate constant data are available for the decarboxylation of larger organic carbonyl radicals in solution (see refs 7–9 and references therein), direct measurements of the rate constant for the decomposition of a gas-phase alkoxy carbonyl radical have not been made to my knowledge. To attempt to fill this gap, a relative rate measurement of the rate constant ratio  $k_4/k_{3a}$  is described herein over the temperature range 297–404 K at  $\sim 1$  atm total pressure. While the rate constant  $k_{3a}$  has not been measured, it can be estimated from similar, although not identical, types of reactions, as will be discussed in Section 3.3.

## 2. EXPERIMENT

The gas chromatography–flame ionization detector (GC/FID) analysis has been described in detail previously.<sup>10</sup> Briefly, a spherical (500 cm<sup>3</sup>), Pyrex reactor was used for ambient-temperature measurements. The relative rate constant experiments were performed using initial mixtures of Cl<sub>2</sub> (purity = 99.7%), ethyl formate (99%), and C<sub>2</sub>H<sub>5</sub>Cl (99.5%) [the kinetic reference species], diluted by N<sub>2</sub> (99.999% min). These mixtures were prepared by partial pressure using a vacuum manifold. Freeze/thaw degassing cycles were performed on condensable reactants. In addition, CF<sub>2</sub>Cl<sub>2</sub> (99%) was included in the reaction mixtures for internal calibration of the GC samples. This molecule does not react with Cl and is thermally stable at the maximum temperature and reaction time of these experiments.<sup>11</sup>

Chlorine atoms were generated by irradiation of the unreacted mixture with UV light peaking near 360 nm from a single Sylvania F6T5 BLB fluorescent lamp. After irradiation for a chosen time at ambient temperature, a portion of the contents of the 500 cm<sup>3</sup> reactor was removed into a 2.5 cm<sup>3</sup> gastight syringe set to 1 cm<sup>3</sup> (Hamilton) using the vacuum manifold. The sample was analyzed by injection into the injector port (373 K) of the gas chromatograph. The presence of the internal calibration species, CF<sub>2</sub>Cl<sub>2</sub>, permitted corrections to be made for uncertainty in the precise amount of sample injected into the GC using the syringe. The mixture in the 500 cm<sup>3</sup> reactor was then irradiated for additional times, and these additional samples were analyzed. All ambient temperature experiments in this reactor were carried out at a total pressure of  $\sim 950$  Torr.

Elevated temperature experiments were performed over the range 297–435 K using a  $\sim 40$  cm<sup>3</sup>, cylindrical, Pyrex reactor (26 mm ID  $\times$   $\sim 7$  cm length) with a thermocouple well along the axis and a Teflon-sealed, glass stopcock attached to a Pyrex capillary tube at the end opposite the thermocouple well. This reactor was placed inside a tube oven, whose lid remained open approximately 6 mm to allow radiation from the fluorescent lamp to enter. The calibration of the chromel–alumel thermocouple was checked in ice and boiling water. The temperature along the axis of the reactor was uniform to  $\pm 1$  K

from the mean. During a reaction, a portion of the unreacted mixture in a storage flask was placed into the high-temperature reactor at a pressure of  $\sim 760$  Torr. The mixture was then irradiated for a chosen time, and a sample of the contents was withdrawn into the gastight syringe using the vacuum manifold, after removing a small amount to purge the low temperature dead volume. Only one irradiation was possible per sample placed into the reactor for the high temperature experiments because of the substantial pressure loss during sampling.

Identification and GC calibration of ethyl formate (Sigma-Aldrich 99%) and the product ethyl chloroformate (Sigma-Aldrich 99%), formed by reaction 1a followed by reaction 3a, were carried out by injecting a known concentration of the pure species into the GC in the presence of the internal calibration species. This provides a determination of the retention time and relative GC/FID response of the two species. The molar responses of both ethyl formate and ethyl chloroformate were the same within experimental error. The retention time of ethyl formate was 6.00 min, and that of ethyl chloroformate was 8.35 min.

A sample of 2-chloroethyl formate was also available from Sigma-Aldrich, but this compound was provided at a purity stated to be “as is” with the predominant impurity being ethyl formate, according to the GC analysis herein. In this case, no calibration of the GC/FID sensitivity was possible but the retention time of 2-chloroethyl formate was observed to be 9.62 min. 1-chloroethyl formate was not available commercially and neither its retention time nor its GC/FID sensitivity could be determined directly. The retention time of this species was deduced from the GC trace during a photolysis experiment. When irradiation of the unreacted mixture was complete, ethyl chloroformate and 2-chloroethyl formate were observed at 297 K. A third GC peak, which was the predominant product peak, was also observed at a retention time of 8.42 min. This peak was assigned to the 1-chloroethyl formate product.

In calculating the product molar yields, the assumption is made that the molar GC/FID responses of all three products are identical to that of ethyl formate. This was verified experimentally for ethyl chloroformate as stated above. The following observations lend support for this assumption in the cases of 1- and 2-chloroethyl formate. In previous experiments using this GC/FID instrument, the response factors of several chlorinated versus nonchlorinated species were measured. These observations showed that CH<sub>3</sub>Cl had the same response factor as CH<sub>4</sub>; C<sub>2</sub>H<sub>5</sub>Cl the same as C<sub>2</sub>H<sub>6</sub>; and CH<sub>3</sub>CHO the same as CH<sub>3</sub>COCl. In every case, substitution of a single Cl for a hydrogen atom produced no measurable change in the FID response to within  $\pm 3\%$ . This lends support to the assumption that 1- and 2-chloroethyl formate will have essentially the same FID response as ethyl formate, and this assumption will be used to calculate yields of these products.

One problem occurred during these experiments that has not been observed previously with analyses using this GC/FID system. When using the high-temperature reactor, the composition of the unreacted mixture in the storage flask used to fill that reactor is analyzed. This composition measurement provides the unreacted composition in the high temperature reactor, because the contents of the unreacted mixture cannot be analyzed after filling. To test this assumption, the high temperature reactor was filled and sampled without irradiation. In the past, this sample always matched the composition in the storage flask to within the experimental error of approximately  $\pm 1.0\%$ . For ethyl formate,

this was not the case. When the unreacted mixture was placed in the reactor in limited tests and sampled without being irradiated, the ethyl formate signal was  $7 \pm 5\%$  larger than observed by analyzing the unreacted mixture in the storage flask. The cause of this effect is unknown, but it undoubtedly causes additional error in determining the product yields. In all product yield calculations, the initial mole fraction of ethyl formate was assumed to be 1.07 times that measured in the flask containing the initial mixture.

### 3.0. RESULTS AND DISCUSSION

**3.1. Rate Constant of Reaction 1.** In a brief set of experiments, the rate constant of reaction 1 (Cl + ethyl formate) was measured at 297 K and  $\sim 950$  Torr relative to that of reaction 2 (Cl + ethyl chloride) for comparison to two previous relative rate measurements of  $k_1/k_2$ .<sup>1,2</sup> Table 1

**Table 1. Initial Conditions and Results for Measurements of the Rate Constant of Reaction 1 Relative to That of Reaction 2 in N<sub>2</sub> at 297 K and 950 Torr (Data Plotted in Figure 1)**

data set	$t_{\text{irr}}^a$ (sec)	Cl <sub>2</sub> <sup>b</sup> (ppm)	C <sub>2</sub> H <sub>5</sub> Cl <sup>b</sup> (ppm)	EF <sup>b</sup> (ppm)	C <sub>2</sub> H <sub>5</sub> Cl <sub>0</sub> /C <sub>2</sub> H <sub>5</sub> Cl <sub>0</sub> <sup>c</sup>	EF <sub>0</sub> /EF <sub>0</sub> <sup>c</sup>	$k_1/k_2^d$
1a	2	1056	188	74	0.663	0.657	1.02
1b	4				0.396	0.372	1.07
1c	6				0.217	0.195	1.07
2a	$\sim 2$	719	241	23	0.841	0.843	0.99
2b	8				0.513	0.518	0.99
3	7	1548	123	157	0.0871	0.0714	1.08

<sup>a</sup>Time of irradiation in the 500 cm<sup>3</sup> reactor. <sup>b</sup>Initial mole fractions of reactants. EF = ethyl formate. Data points with same number but different letter designation were obtained from the same initial mixture. <sup>c</sup>Ratio of the final ( $t$ ) to the initial (0) concentrations after irradiation is complete. <sup>d</sup>Ratio of the rate constant for reaction of Cl with ethyl formate to that for reaction with C<sub>2</sub>H<sub>5</sub>Cl.

presents the initial reactant concentrations and values of  $c_t/c_0$  for both ethyl formate and ethyl chloride after irradiation for a time  $t$ . In Table 1, each numbered data set was obtained from the same initial mixture placed into the 500 cm<sup>3</sup> reactor. In the case of data set 1, this mixture was irradiated three times successively, resulting in the three total irradiation times represented by the letter designations 1a, 1b, and 1c for data set 1 in Table 1. The total irradiation time for each data point is presented as  $t_{\text{irr}}$  in the table. The three data sets (1, 2, and 3) were obtained on three separate days spanning a month and show satisfactory consistency. The initial concentrations of the reactants also varied across the data sets with no significant change in the measured rate constant ratios.

According to the equation for relative rate determinations:  $\log_{10}\{[\text{ethyl formate}]_t/[\text{ethyl formate}]_0\}/\log_{10}\{[\text{ethyl chloride}]_t/[\text{ethyl chloride}]_0\} = k_1/k_2$ . The subscript  $t$  represents the mole fraction after irradiation for time  $t$ , and subscript 0 represents the initial mole fraction. Figure 1 presents a log–log plot of the six data points presented in Table 1 at 297 K. The slope of the least-squares fit to the data points is calculated to be  $1.09 \pm 0.05$ , where the error limit includes the statistical  $2\sigma$  for the six data points ( $\pm 0.025$ ) plus an additional factor of 2 because the data set is very limited. The value of  $k_1/k_2$  agrees satisfactorily with that determined by Balaganesh et al.<sup>1</sup> ( $k_1/k_2 = 1.19 \pm 0.09$ ) and by Wallington et al.<sup>2</sup> ( $k_1/k_2 = 1.13 \pm 0.10$ ). This rate constant measurement was performed primarily to show that the current experiments agreed with the previous

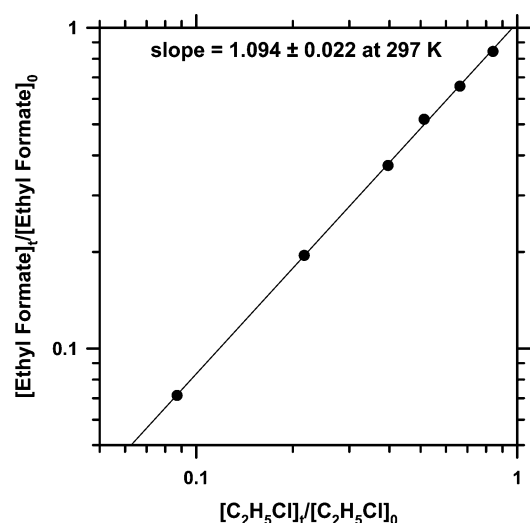


**Figure 1.** Plot of the  $\log_{10}$  of the fractional consumption of ethyl formate versus that of the reference compound ethyl chloride. The slope of the resultant line =  $k_1/k_2 = 1.09 \pm 0.025$ , where the error limit represents the statistical  $2\sigma$  from a least-squares fit. Because the data are very limited, a larger error limit  $k_1/k_2 = 1.09 \pm 0.05$  is more appropriate.

measurements, not to provide a more accurate measurement of  $k_1/k_2$ , and, therefore, limited data were taken.

**3.2. Experimental Product Yields.** Table 2 presents selected experiments during which the yields of the three stable products formed by reaction 1 followed by reaction 3 (ethyl chloroformate, 1-chloroethyl formate, and 2-chloroethyl formate) were determined. No ethyl chloride was present in these mixtures because the rate constant of reaction 1 was not being determined. These products are formed from the reaction of the molecular chlorine present in the initial mixture with the free radical species produced by the H atom abstraction reactions 1a–1c. The yields of the free radical species can be determined from the yields of the three chlorides produced quantitatively from them by reactions 3a–3c. This table presents the initial reactant concentrations present in each mixture, the reactor temperature and pressure, and the irradiation time. The number designations again indicate experiments having the same initial mixture, while the letter designations indicate different irradiation times. The fractional consumption of the ethyl formate ( $EF_t/EF_0$ ) is also presented in Table 2. The molar percentage yields of each of the three chloride products ( $100[\text{moles product}]/[\text{moles of ethyl formate consumed}]$ ) are tabulated along with the C<sub>2</sub>H<sub>5</sub>Cl molar yield, which is formed from the C<sub>2</sub>H<sub>5</sub> radicals produced by the decarboxylation of the C<sub>2</sub>H<sub>5</sub>OC(=O) radical at elevated temperature via reaction 4. These yields are labeled raw yields in subsequent discussions and have been corrected for secondary consumption as described below. Because the C<sub>2</sub>H<sub>5</sub>OC(=O) radical begins to decompose according to reaction 4 at elevated temperature, the actual yield of the C<sub>2</sub>H<sub>5</sub>OC(=O) radical produced by reaction 1a is obtained from the sum of the molar yields of the C<sub>2</sub>H<sub>5</sub>Cl and C<sub>2</sub>H<sub>5</sub>OC(=O)Cl product species. This sum is also presented in Table 2. Reaction 4 will be discussed in detail in section 3.3. The FID sensitivities for neither CH<sub>3</sub>CHClOC(=O)H nor CH<sub>2</sub>ClCH<sub>2</sub>OC(=O)H could be determined. It is assumed that they are identical to that of ethyl formate based on the discussion in the Experiment section.

**Table 2. Results and Initial Conditions for Selected Experiments in the Study of the Products Formed during Reaction 1 (Cl + ethyl formate)<sup>a</sup>**

Data	$t_{\text{irr}}^b$ (sec)	$T^b$ (K)	$P^b$ (torr)	EF <sup>c</sup> /EF <sub>0</sub>	EF <sub>0</sub> <sup>d</sup> (ppm)	Cl <sub>2</sub> <sup>d</sup> (ppm)	[Cl <sub>2</sub> ] <sub>av</sub> <sup>d</sup> (ppm)	C <sub>2</sub> H <sub>5</sub> Cl <sup>e</sup> (%)	ECIF <sup>e</sup> (%)	1-CIEF <sup>e</sup> (%)	2-CIEF <sup>e</sup> (%)	C <sub>2</sub> H <sub>5</sub> Cl + ECIF (%) <sup>e</sup>	ΣC <sup>f</sup> (%)	$k_4/k_{3a}^g$ molecules cm <sup>-3</sup>
1	lost	297	950	0.484	200	444	392	~0.24 <sup>h</sup>	19.3	51.5	5.8	19.5	76.8	1.38 × 10 <sup>14</sup>
2a	2.3	297	950	0.524	214	724	673	~0.15 <sup>h</sup>	19.7	61.6	7.5	19.7	89	1.44 × 10 <sup>14</sup>
2b	4.8			0.277			647	~0.16 <sup>h</sup>	19.8	67.5	8.1	19.8	95.4	1.65 × 10 <sup>14</sup>
3	1.8	297	950	0.469	210	703	648	~0.22 <sup>h</sup>	20.2	51.4	6.4	20.4	78.2	2.00 × 10 <sup>14</sup>
4a	15	320	710	0.83	205	474	456	1.68	20.2	51.4	9.2	21.9	82.5	8.12 × 10 <sup>14</sup>
4b	40	322	760	0.63			436	1.56	18.4	46.5	7.6	20.0	74.1	8.42 × 10 <sup>14</sup>
4c	80	321	760	0.27			399	1.62	19.4	54.3	9.0	21.0	84.3	7.60 × 10 <sup>14</sup>
5a	30	335	760	0.74	237	458	427	3.34	15.1	38.8	7.1	18.5	64.4	2.07 × 10 <sup>15</sup>
5b	53	335	720	0.50			398	3.85	16.6	47.4	9.2	20.5	75.1	1.91 × 10 <sup>15</sup>
5c	75	335	760	0.40			387	3.75	16.4	47.9	8.7	20.2	76.8	1.94 × 10 <sup>15</sup>
6a	32	367	760	0.80	214	431	416	9.18	7.5	35.0	7.6	16.7	59.3	1.02 × 10 <sup>16</sup>
6b	75	366	725	0.42			372	12.4	8.8	51.0	11.3	21.2	89.2	1.00 × 10 <sup>16</sup>
6c	120	366	765	0.28			354	11.8	8.1	49.0	9.1	19.9	78.0	1.04 × 10 <sup>16</sup>
7a	13.5	383	660	0.88	212	443	431	19.0	7.9	56.4	13.8	26.9	96.6	1.72 × 10 <sup>16</sup>
7b	21	383	720	0.76			433	15.9	5.5	40.4	11.0	21.4	72.8	2.21 × 10 <sup>16</sup>
7c	37	383	770	0.35			404	14.6	6.0	44.0	10.3	20.6	72.5	1.91 × 10 <sup>16</sup>
8a	18	401	760	0.67	103	388	371	16.8	2.9	38.1	7.9	19.8	65.3	3.88 × 10 <sup>16</sup>
8b	38	402	780	0.48			361	18.7	3.0	46.4	10.3	21.7	78.4	4.22 × 10 <sup>16</sup>
8c	60	400	720	0.21			347	18.9	2.7	55.9	11.3	21.6	88.8	4.22 × 10 <sup>16</sup>
10a	8	403	760	0.72	206	790	761	17.6	5.4	48.0	14.0	23.0	85.0	4.54 × 10 <sup>16</sup>
10b	37	404	770	0.22			710	21.2	4.9	56.7	14.4	26.1	95.2	5.63 × 10 <sup>16</sup>
11	60	434		0.35	206	445		20.7	0 <sup>i</sup>	48.5	12.3	20.7	81.5	<sup>i</sup>

<sup>a</sup>EF = ethyl formate; ECIF = ethyl chloroformate; 1-CIEF = 1-chloroethyl formate; 2-CIEF = 2 chloroethyl formate. All of the data points used to determine  $k_4/k_{3a}$  are included in this table. <sup>b</sup> $t_{\text{irr}}$  (sec) = irradiation time in sec.  $T$  = reactor temperature;  $P$  = reactor pressure. <sup>c</sup>Fractional consumption of ethyl formate during irradiation. <sup>d</sup>Initial mole fractions of ethyl formate and Cl<sub>2</sub>. [Cl<sub>2</sub>]<sub>av</sub> represents the average Cl<sub>2</sub> mole fraction which accounts for loss during irradiation (see text). <sup>e</sup>Raw product yields in mole percent corrected for secondary consumption. Not corrected to 100% total carbon yield (see Section 3.2). Note C<sub>2</sub>H<sub>5</sub>Cl + ECIF represents the yield of the ethoxy carbonyl radical [C<sub>2</sub>H<sub>5</sub>OC(=O)] produced in reaction 1. <sup>f</sup>Total apparent carbon recovery in mole percent. <sup>g</sup> $k_4/k_{3a} = [\text{C}_2\text{H}_5\text{Cl}][\text{Cl}_2]_{\text{av}}/[\text{ECIF}]$  (see text). <sup>h</sup>Approximate C<sub>2</sub>H<sub>5</sub>Cl yield near noise limit. Data points not included in the fit to the data in Figure 4. <sup>i</sup>No ECF visible above the noise in GC trace. Therefore,  $k_4/k_{3a}$  cannot be determined.

The molar yields of the chlorinated products presented in Table 2 have been corrected for secondary consumption by chlorine atoms using a chemical model entered into the Acuchem kinetics solver.<sup>12</sup> The rate constants for the reactions of Cl with ethyl chloroformate, 1-chloroethyl formate, and 2-chloroethyl formate necessary to calculate this correction have not been determined previously. Therefore, approximate rate constants for the reaction of Cl with ethyl chloroformate ( $k_6$ ) and with 2-chloroethyl formate ( $k_7$ ) relative to that of ethyl formate were determined in a single experiment at 297 K.

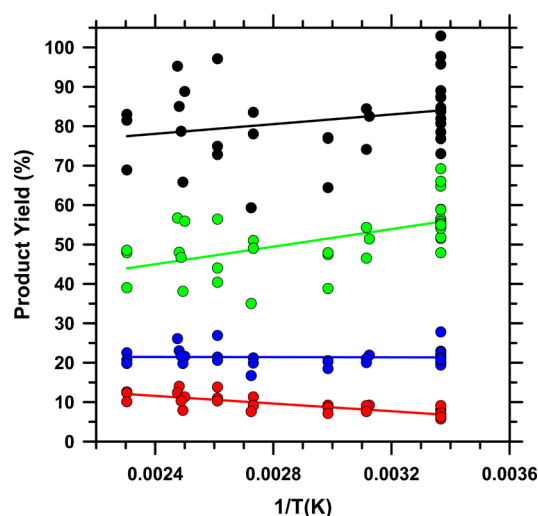
The rate constant of 1-chloroethyl formate with Cl ( $k_8$ ) could not be determined since the compound was not available commercially as stated in the Experiment section. The rate constant ratios determined at 297 K are  $k_6/k_1 = 0.25 \pm 0.06$ ; and  $k_7/k_1 = 0.27 \pm 0.06$ . The rate constant ratio  $k_8/k_1$  was assumed to be equal to  $k_7/k_1$  for the purpose of calculating the correction for secondary consumption. Approximate relative rate ratios were also determined at 410 K for ethyl chloroformate and for 2-chloroethyl formate during a single experiment. The results showed that  $k_6/k_1$  at 297 and 410 K were identical to within experimental error. The ratio  $k_7/k_1 = (0.34 \pm 0.1)$  at 410 K was slightly higher than at 297 K (although indistinguishable within the error limits), and  $k_8/k_1$  was again assumed equal to  $k_7/k_1$  at 410 K. For the purpose of correcting for secondary consumption, both  $k_7/k_1$  and  $k_8/k_1$  were set equal to 0.34 at all temperatures at and above 400 K and 0.25 for temperatures below 400 K. Because the secondary corrections are typically <20% (maximum correction =35%),

uncertainty in the secondary consumption correction is estimated to produce errors less than the experimental data scatter. Note that data points 4a and 4c in Table 2 have very different fractional consumptions of ethyl formate (0.83 and 0.27, respectively). The product yields are identical to within experimental error, providing support for the validity of the secondary consumption corrections.

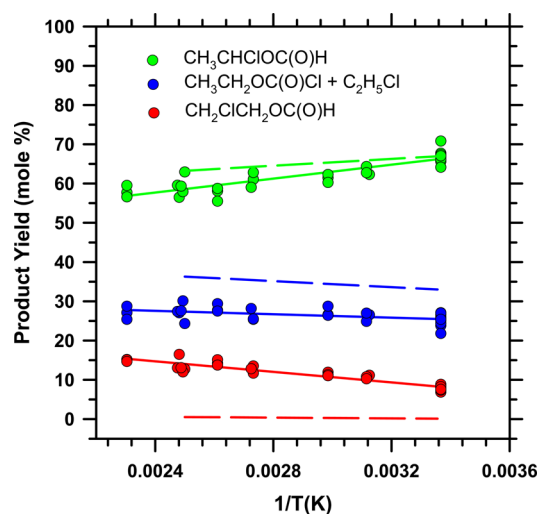
As shown by data points 1–3 at 297 K in Table 2, the total carbon recovery in these ambient-temperature experiments is between 77% and 95%. The near 100% carbon recovery supports the assumption that the GC/FID response of all three products is equal to that of ethyl formate. In the high temperature reactor, the carbon recovery varies from 60% to 90%, somewhat lower than at ambient temperature probably because of uncertainty in measuring the initial mole fraction of ethyl formate as discussed in the Experiment section.

Figure 2 presents the measured raw product yields, corrected for secondary consumption as described above in this section, and the total carbon recovery determined in these experiments. The line through each set of individual product data represents a least-squares fit to those points. For these plots, the data scatter is relatively large. A substantial contribution to this uncertainty likely results from the scatter in the total carbon recovery, which in turn reflects the uncertainty in the initial ethyl formate mole fraction in the reactor as discussed at the end of the Experiment section.

In Figure 3, the consumption of ethyl formate is assumed to be equal to the sum of the product mole fractions, thereby



**Figure 2.** Plot of the raw (corrected for secondary consumption but not corrected to 100% carbon recovery) molar yield of the chlorinated products from reaction 1 as a function of reciprocal temperature from 297 to 434 K. Red symbols represent 2-chloroethyl formate; blue symbols represent ethyl chloroformate; and green symbols represent 1-chloroethyl formate. The black symbols represent the total carbon recovery in mole percent for each experiment.



**Figure 3.** Plot of the product yields (corrected for secondary consumption) calculated using the sum of the products to represent the mole fraction of ethyl formate consumed to reduce the data scatter (see text). The yield of the  $\text{CH}_3\text{CH}_2\text{OC}(=\text{O})$  radical is obtained from the sum of the molar product yields,  $\text{CH}_3\text{CH}_2\text{OC}(=\text{O})\text{Cl} + \text{C}_2\text{H}_5\text{Cl}$ , because the radical can decompose in addition to reacting with  $\text{Cl}_2$  (see text). Dashed lines represent the ab initio calculations of Balaganesh et al.<sup>1</sup> (see text).

forcing the total carbon recovery to be 100%. This is equivalent to dividing each raw product yield (corrected for secondary consumption) presented in Table 2 by the total fractional carbon recovery for that individual experiment. As seen in Figure 3, this reduces the data scatter of the product yields, by eliminating the uncertainty in the initial mole fraction of ethyl formate, which will affect the calculated yields. Figures 2 and 3 both show that the major chlorinated product is 1-chloroethyl formate followed by ethyl chloroformate and 2-chloroethyl formate, which has the lowest yield. In Figure 3, the yield of

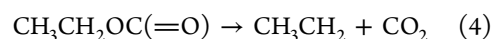
each chlorinated product is again fitted to a least-squares expression shown by the solid colored lines.

The yields of the precursor radicals formed by reactions 1a–1c predicted by Balaganesh et al.<sup>1</sup> are shown by the dashed lines in Figure 3 using the same color code. The predicted yield of the  $\text{CH}_3\text{CHOC}(=\text{O})\text{H}$  radical [67%] at 298 K agrees well with the measured yield of 1-chloroethyl formate [ $67 \pm 5\%$ ]. The predicted yield of the  $\text{CH}_3\text{CH}_2\text{OC}(=\text{O})$  radical [33%] is in reasonable agreement with the [ $25 \pm 3\%$ ] yield of ethyl chloroformate measured herein. The small experimental temperature dependencies for the  $\text{CH}_3\text{CHClOC}(=\text{O})\text{H}$  and  $\text{CH}_3\text{CH}_2\text{OC}(=\text{O})\text{Cl}$  yields are also similar to those predicted for their free radical precursors by Balaganesh et al. However, the yield predicted for the  $\text{CH}_2\text{CH}_2\text{OC}(=\text{O})\text{H}$  radical [0.11% at 298 K] by Balaganesh et al is nearly a factor of 100 smaller than the [ $8 \pm 2\%$ ] yield measured experimentally for  $\text{CH}_2\text{ClCH}_2\text{OC}(=\text{O})\text{H}$ . The predicted yield seems low for abstraction of a hydrogen atom from a  $\text{CH}_3$  group. As an example, site specific rate constants have been measured for the reaction  $\text{Cl} + \text{CH}_3\text{CH}_2\text{OH}$  by Taatjes et al.<sup>13</sup> At 295 K, the ratio of the rate constants for abstraction at the two ethyl group sites is observed to be  $k_{\text{CH}_3}/k_{\text{CH}_2} = 0.075 \pm 0.02$ , while no measurable reaction occurs at the hydroxyl hydrogen. While ethanol is not structurally identical to ethyl formate, it does contain an ethoxy group as does ethyl formate. If we assume that the ethoxy groups behave similarly in the two molecules regarding their site specificity toward Cl atom abstraction, the ratio in ethyl formate would also be of the order of  $k_{\text{CH}_3}/k_{\text{CH}_2} = 0.075 \pm 0.02 = k_{1c}/k_{1b}$ . Based on the yield of 1-chloroethyl formate determined herein (67%), we would predict that the yield of 2-chloroethyl formate will be  $(0.075 \pm 0.02) \times 67 = (5 \pm 1.4)\%$ , indicating that abstraction at the 2-ethyl position should not be negligible. In addition, in a measurement of the product branching fraction for the reaction  $\text{Cl} + \text{CH}_3\text{OC}(=\text{O})\text{H}$  Wallington et al.<sup>14</sup> observed that 45% occurred by hydrogen abstraction from the methyl group and 65% by abstraction of the formyl hydrogen. This result also shows that abstraction from a primary hydrogen is not likely to be negligibly small.

One previous measurement of the product yields formed from channels 1a–1c of reaction 1 carried out at 298 K has been published using totally different chemistry to trap these radicals.<sup>15</sup> These authors determined that  $62 \pm 7\%$  of reaction 1 proceeded through channel 1b in good agreement with the data in Figure 3 and  $44 \pm 5\%$  through channel 1a, which is larger than measured herein. These authors did not observe any products attributable to channel 1c, but they stated that  $(2 \pm 1)\%$  of reaction 1 could proceed by 1c based on the measured yields and error limits of the products observed from channels 1a and 1b quoted above. Their method of obtaining this estimate for the yield from channel 1c was not described.

### 3.3. Decomposition Rate Constant of $\text{CH}_3\text{CH}_2\text{OC}(=\text{O})$ .

The ethoxy carbonyl radical [ $\text{CH}_3\text{CH}_2\text{OC}(=\text{O})$ ] formed by reaction 1a has two subsequent reaction channels that form final products under the experimental conditions tested. It can react with molecular chlorine in the mixture to form  $\text{CH}_3\text{CH}_2\text{OC}(=\text{O})\text{Cl}$  via reaction 3a, or it can decompose at elevated temperature to  $\text{CO}_2$  and ethyl radicals by reaction 4. The ethyl radicals formed in the decarboxylation reaction will be trapped by reaction with  $\text{Cl}_2$  to form  $\text{C}_2\text{H}_5\text{Cl}$  via reaction 5





Equations 3a, 4, and 5 show that in the decomposition experiments the  $\text{CH}_3\text{CH}_2\text{OC}(=\text{O})$  radical can form two final chlorinated organic products,  $\text{CH}_3\text{CH}_2\text{OC}(=\text{O})\text{Cl}$  and  $\text{CH}_3\text{CH}_2\text{Cl}$ . The ethyl chloride product is the sole hydrocarbon product formed from the decomposition reaction after the  $\text{C}_2\text{H}_5$  radical is trapped by  $\text{Cl}_2$  via reaction 5. By analyzing kinetic eqs 3a, 4, and 5, an expression for  $k_4/k_{3a}$  is obtained. This rate constant ratio for the two reaction channels of the  $\text{CH}_3\text{CH}_2\text{OC}(=\text{O})$  radical can be calculated from the measured final chlorinated product yields (in mole percent),  $Y[\text{C}_2\text{H}_5\text{Cl}]$  and  $Y[\text{C}_2\text{H}_5\text{OC}(=\text{O})\text{Cl}]$  presented for each data point in Table 2.

$$\begin{aligned} k_4/k_{3a} &= Y[\text{C}_2\text{H}_5\text{Cl}][\text{Cl}_2]_{\text{av}}/Y[\text{C}_2\text{H}_5\text{OC}(=\text{O})\text{Cl}] \\ &= (A_4/A_{3a})e^{-[(Ea(4)-Ea(3a))/RT]} \end{aligned}$$

In this equation, a new expression,  $[\text{Cl}_2]_{\text{av}}$ , appears. Because  $\text{Cl}_2$  is consumed during reactions 1, 3, and 5, the average  $\text{Cl}_2$ , defined as  $[\text{Cl}_2]_{\text{av}} = \{[\text{Cl}_2]_0 + [\text{Cl}_2]_t\}/2$ , is used in the calculation of this rate constant ratio and is also presented in Table 2. Examining kinetic eqs 1, 3, 4, and 5, it can be seen that one  $\text{Cl}_2$  molecule is consumed for each ethyl formate molecule that reacts. The removal of chlorine during the secondary consumption of products discussed earlier will be smaller and is not included in  $[\text{Cl}_2]_{\text{av}}$ . One fact must be emphasized in these decomposition experiments. Both ethyl chloride and ethyl chloroformate are calibrated from pure samples. Therefore, there are no assumptions made concerning the FID response for these species that could contribute to uncertainty in the expression for  $k_4/k_{3a}$ . Also, since the ratio of the yields of these two species is used in this expression, it will not be affected by uncertainty in the initial ethyl formate mole fraction used in the calculation of the yields, which was discussed in the Experiment section. Table 2 presents all of the data points generated for measuring the rate constant ratio  $k_4/k_{3a}$  as a function of temperature. The thermal stabilities of  $\text{C}_2\text{H}_5\text{Cl}$  and  $\text{CH}_3\text{CH}_2\text{OC}(=\text{O})\text{Cl}$  were checked in the high temperature reactor. No measurable decomposition (<2%) was observed for either species at temperatures up to 432 K for reaction times encountered in these experiments. This agrees with shock tube experiments on  $\text{CH}_3\text{CH}_2\text{OC}(=\text{O})\text{Cl}$  by Saito et al.<sup>16</sup>

Assuming a positive activation energy for the decomposition reaction 4 and near zero activation energy for reaction 3a as discussed below, the yield of  $\text{C}_2\text{H}_5\text{Cl}$  should increase and that of  $\text{CH}_3\text{CH}_2\text{OC}(=\text{O})\text{Cl}$  should decrease as the temperature of the reactor increases while the sum of the two yields remains constant. Table 2 and Figure 4 show that this is the case. At ambient temperature, the raw (corrected for secondary consumption but not corrected to 100% carbon recovery)  $\text{C}_2\text{H}_5\text{Cl}$  yield, formed from decarboxylation reaction 4, is ~0.2%, while the raw yield of  $\text{CH}_3\text{CH}_2\text{OC}(=\text{O})\text{Cl}$  is ~20%. At 435 K,  $\text{C}_2\text{H}_5\text{Cl}$  has risen to ~20%, and  $\text{CH}_3\text{CH}_2\text{OC}(=\text{O})\text{Cl}$  is below the GC/FID detection limit of ~0.1%. The sum of these two product yields remains constant at ~20% over the 297–434 K temperature range, as required if these two species are the sole products formed from the  $\text{CH}_3\text{CH}_2\text{OC}(=\text{O})$  radical. Figure 4 plots the yields of  $\text{CH}_3\text{CH}_2\text{OC}(=\text{O})\text{Cl}$  and  $\text{C}_2\text{H}_5\text{Cl}$  (now corrected to 100% total carbon recovery as described above). This plot shows that there is a smooth transition from  $\text{CH}_3\text{CH}_2\text{OC}(=\text{O})\text{Cl}$  at ambient to  $\text{C}_2\text{H}_5\text{Cl}$  as

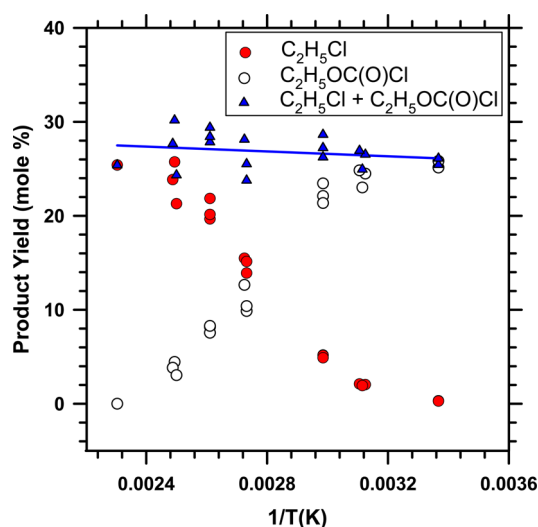


Figure 4. Molar yields of the products  $\text{C}_2\text{H}_5\text{OC}(=\text{O})\text{Cl}$  (open circles) and  $\text{C}_2\text{H}_5\text{Cl}$  (red circles) plotted as a function of reciprocal temperature. Also included in the figure is the sum of the two products (blue triangles). All yields have been corrected to 100% carbon recovery as described in section 3.2.

the temperature increases to 435 K with a constant sum of 27 ± 3%.

The slope of a plot of  $\ln[k_4/k_{3a}]$  versus  $1/T$  equals  $(Ea_4 - Ea_{3a})/R$ , where  $Ea_4$  represents the activation energy of reaction 4 and  $Ea_{3a}$  is the activation energy of reaction 3a.  $R$  is the gas constant ( $= 1.987 \text{ cal K}^{-1} \text{ mol}^{-1}$ ). Thus, the data in Table 2 can be used to determine an approximate value for the activation energy of reaction 4. The value is approximate because obtaining  $Ea_4$  from the slope requires knowledge of the activation energy of reaction 3a, which has not been measured. However, rate constant expressions for four organic radical abstraction reactions with  $\text{Cl}_2$  have been measured, and these rate constants can assist in estimating a value for  $Ea_{3a}$ . The rate expressions for these four reactions are presented in Table 3 along with the rate constants derived from them at two temperatures (297 and 400 K), which span the range used in the current experiments. The examples include the reactions of  $\text{Cl}_2$  with the acetyl and formyl radicals, which are directly related to the  $\text{C}_2\text{H}_5\text{OC}(=\text{O})$  radical by the free radical site present on the carbon atom of the carbonyl group. The activation energies of these two radical reactions are zero to within experimental error. Ethyl and methoxy methyl radicals are also included in the table and have activation energies of 0 and  $-700 \text{ cal mol}^{-1}$ , respectively. Of these four examples, the closest analogue to the ethoxy carbonyl radical is the acetyl (or methyl carbonyl) radical. For this radical,  $Ea = -140 \pm 210 \text{ cal mol}^{-1}$  based on the data of Maricq and Szenté<sup>17</sup> (212–357 K) and Gierczak et al.<sup>18</sup> (253–384 K). Taking into account the activation energies of the other organic free radicals included in Table 3 and their errors, the best estimate available for  $Ea_{3a}$  is  $-140 \pm 500 \text{ cal mol}^{-1}$ . The pre-exponential factor  $A_{3a}$  can be estimated to be  $1.6 \times 10^{-11} \text{ s}^{-1}$  based on the average of the  $A$  factors for the four chlorination reactions. Again taking into account the other reactions in Table 3, a reasonable estimate for the error in  $A_{3a}$  is ± a factor of 2, yielding  $A_{3a} = 1.6 (+1.6, -0.8) \times 10^{-11} \text{ s}^{-1}$ .

Figure 5 presents a plot of  $\log_{10}[k_4/k_{3a}]$  versus  $1/T$  from 297 to 404 K. Values of  $k_4/k_{3a}$  could not be determined at higher temperature under the experimental conditions studied

Table 3. Rate Constants for Four Reactions of Organic Free Radicals with Cl<sub>2</sub>

reaction	rate constant	297 K <sup>a</sup>	400 K <sup>a</sup>	citation
1. CH <sub>3</sub> C(=O) + Cl <sub>2</sub>	$2.8 \times 10^{-11} e^{-(93 \pm 180)/RT}$	$2.4 \times 10^{-11}$	$2.5 \times 10^{-11}$	17 <sup>b</sup>
	$2.2 \times 10^{-11} e^{+(190 \pm 240)/RT}$	$3.0 \times 10^{-11}$	$2.8 \times 10^{-11}$	18 <sup>c</sup>
2. HCO + Cl <sub>2</sub>	$6.3 \times 10^{-12} e^{-(0 \pm 500)/RT}$	$6.3 \times 10^{-12}$	$6.3 \times 10^{-12}$	19
	$7.6 (\pm 0.7) \times 10^{-12}$	$7.6 \times 10^{-12}$	-	20
3. CH <sub>3</sub> OCH <sub>2</sub> + Cl <sub>2</sub>	$1.8 \times 10^{-11} e^{+(715 \pm 240)/RT}$	$6.0 \times 10^{-11}$	$4.4 \times 10^{-11}$	21
4. C <sub>2</sub> H <sub>5</sub> + Cl <sub>2</sub>	$1.26 \times 10^{-11} e^{+(131 \pm 50)/RT}$	$1.5 \times 10^{-11}$	$1.6 \times 10^{-11}$	22

<sup>a</sup>Rate expression evaluated at stated temperature. <sup>b</sup>Estimated error  $\pm 25\%$  (297–400 K). <sup>c</sup>Estimated error  $\pm 20\%$  (297–400 K).

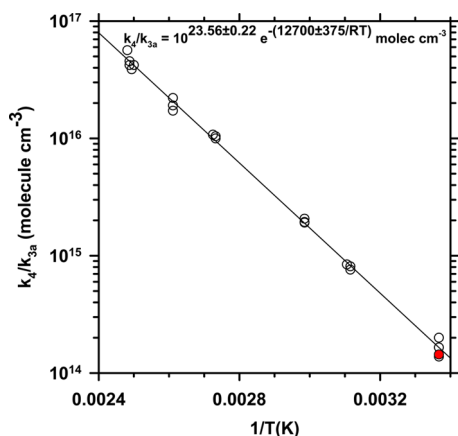


Figure 5. Plot of the expression  $\log_{10}[k_4/k_{3a}]$  versus  $1/T$ , where  $k_4/k_{3a} = Y[C_2H_5Cl][Cl_2]_{av}/Y[C_2H_5OC(=O)Cl]$ . The red filled circle is the best data point at 297 K. The 297 K data points are not included in the fit as discussed in the text.

because, as shown in both Table 2 and Figure 4 and discussed above, at a temperature of 434 K, no measurable ethyl chloroformate remains, precluding calculations of  $k_4/k_{3a}$  at and above this temperature. This indicates that essentially all of the C<sub>2</sub>H<sub>5</sub>OC(=O) radicals decompose to C<sub>2</sub>H<sub>5</sub> + CO<sub>2</sub> during the experiment to within experimental error at 434 K. Initial composition ranges for ethyl formate and Cl<sub>2</sub> are (103–237 ppm) and (388–790 ppm), respectively, and the ethyl formate consumption varies from 12% to 80%. All data points lie within  $\pm 15\%$  from the least-squares fit shown by the solid line, while the value of  $k_4/k_{3a}$  changes by approximately a factor of  $\sim 300$ .

The data points at 297 K were not used in the fit because the ethyl chloride signal was barely above the noise level for most data and will have larger error limits than the measurements at elevated temperature. The best ambient temperature data point is that colored red (and labeled 2b in Table 2), in which over 70% of the ethyl formate was consumed, thereby forming more product and producing a larger GC/FID signal. Even though they were not used in the fit, the ambient temperature data points fall on the least-squares fit to the higher temperature data.

A least-squares fit to the data in Figure 5 yields the expression below. The error limits are  $2\sigma$ :

$$k_4/k_{3a} = 10^{23.56 \pm 0.22} e^{-(12700 \pm 375)/RT} \text{ molecules cm}^{-3}$$

Note that the error limits are correlated in this expression. When used to calculate the error in the ratio  $k_4/k_{3a}$ , a plus [or minus] sign in the A factor error must be used with the corresponding plus [or minus] sign in the activation energy error to match the observed data scatter. Based on the earlier discussion of an estimate for the activation energy of reaction 3a ( $E_{a3a} = -140 \pm 500 \text{ cal mol}^{-1}$ ), the activation energy of reaction 4 (CH<sub>3</sub>CH<sub>2</sub>OC(=O) → CO<sub>2</sub> + C<sub>2</sub>H<sub>5</sub>) is calculated to be  $E_{a4} = 12560 \pm 875 \text{ cal mol}^{-1}$  over the range  $T = 297\text{--}404 \text{ K}$ . The pre-exponential factor in the relative rate constant ratio is equal to the ratio of the A factors,  $A_4/A_{3a}$ :

$$\begin{aligned} A_4/A_{3a} &= 10^{23.56 \pm 0.22} \\ &= 3.6(+2.5, -1.5) \times 10^{23} \text{ molecules cm}^{-3} \end{aligned}$$

Table 4. Non-Arrhenius Ab Initio Rate Constant Expressions for Reaction 9 and the Rate Constants Calculated from Them at Two Temperatures Compared to the Measured Arrhenius Rate Constant for  $k_4$

rate constant (s <sup>-1</sup> ) <sup>a</sup>	Arrhenius expression <sup>b</sup>	297 K	400 K	ref.	conditions
	$5.8 \times 10^{12} e^{-12700/RT}$	$2.6 \times 10^3$	$6.7 \times 10^5$	<sup>c</sup>	$\sim 1 \text{ atm, N}_2$
$7.20 \times 10^{15} T^{-1.65} e^{-12071/RT}$	$8.81 \times 10^{10} e^{-10932/RT}$	$7.8 \times 10^2$	$9.4 \times 10^4$	6	1 atm, N <sub>2</sub>
$2.06 \times 10^{17} T^{-1.79} e^{-13439/RT}$	$9.66 \times 10^{11} e^{-12204/RT}$	$1.0 \times 10^3$	$2.1 \times 10^5$	6	10 atm
$8.59 \times 10^{17} T^{-1.72} e^{-14572/RT}$	$6.46 \times 10^{12} e^{-13385/RT}$	$9.1 \times 10^2$	$3.1 \times 10^5$	6	100 atm
$5.92 \times 10^{10} T^{0.78} e^{-13340/RT}$	$1.24 \times 10^{13} e^{-13880/RT}$	$7.7 \times 10^2$	$3.4 \times 10^5$	6	$k_{\infty}$
$1.55 \times 10^{12} T^{0.514} e^{-15182/RT}$	$5.25 \times 10^{13} e^{-15536/RT}$	$1.9 \times 10^2$	$1.7 \times 10^5$	3	<sup>d</sup>
$2.33 \times 10^{11} T^{0.546} e^{-13600/RT}$	$9.81 \times 10^{12} e^{-13976/RT}$	$5.1 \times 10^2$	$2.3 \times 10^5$	24	<sup>d</sup>
$1.89 \times 10^9 T^{0.13} e^{-7974/RT}$	$4.60 \times 10^9 e^{-8062/RT}$	$5.4 \times 10^3$	$1.8 \times 10^5$	23	1 atm
$1.06 \times 10^{10} T^{0.18} e^{-8378/RT}$	$3.63 \times 10^{10} e^{-8500/RT}$	$2.0 \times 10^4$	$8.2 \times 10^5$	23	10 atm
$1.25 \times 10^{16} T^{-1.83} e^{-11341/RT}$	$4.45 \times 10^{10} e^{-10080/RT}$	$1.7 \times 10^3$	$1.4 \times 10^5$	25	1 atm
$1.04 \times 10^{18} T^{-2.1} e^{-12827/RT}$	$5.82 \times 10^{11} e^{-11380/RT}$	$2.4 \times 10^3$	$3.5 \times 10^5$	25	10 atm
$8.69 \times 10^{17} T^{-1.81} e^{-13657/RT}$	$3.55 \times 10^{12} e^{-12410/RT}$	$2.6 \times 10^3$	$5.9 \times 10^5$	25	100 atm

<sup>a</sup>Ab initio expressions derived for  $k_9$ . <sup>b</sup>Arrhenius expressions calculated from the non-Arrhenius ab initio rate constants in column 1 over the range 297–404 K. First line is  $k_4$  for CH<sub>3</sub>CH<sub>2</sub>OC(=O) decarboxylation derived from this work. <sup>c</sup>Experimental  $k_4$  for CH<sub>3</sub>CH<sub>2</sub>OC(=O) decarboxylation derived from this work. Estimated error in the rate constant is a factor of 2 over the 297–404 K range studied (see text). Error in  $E_{a4}$  is estimated to be  $\pm 850 \text{ cal mol}^{-1}$  (see text). <sup>d</sup>Pressure for ab initio calculation not stated.

Inserting the estimate for  $A_{3a}$  presented above ( $A_{3a} = 1.6[+1.6, -0.8] \times 10^{-11}$ ) into the expression for  $A_4/A_{3a}$ , the value of  $A_4$  is calculated to be  $5.8(+7.0, -3.8) \times 10^{12} \text{ s}^{-1}$ . The error limits for  $A_4$  are obtained by propagating the individual errors for  $A_4/A_{3a}$  and  $A_{3a}$  using the quadrature formula for products. In this case this is an approximation since the error in  $A_{3a}$  is only an educated guess rather than a statistical  $2\sigma$ . However, it is the best estimate for the errors that can be obtained. This is a reasonable  $A$  factor range for a first-order decomposition reaction. The final best expression for the temperature-dependent rate constant  $k_4$  is

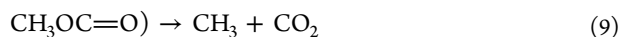
$$k_4 = 5.8(+7.0, -3.8) \times 10^{12} e^{-(12560 \pm 875)/RT} \text{ s}^{-1}$$

In this expression, there is also some unknown degree of correlation between the errors in the  $A$  and  $E_a$  expressions as described above. This uncertainty in the error limits makes this expression less accurate for comparing to the ab initio calculations than the measured value of  $k_4/k_{3a}$ .

Fortunately, the uncertainty in  $k_4$  within the temperature range in which  $k_4/k_{3a}$  was determined (297–404 K) can be estimated more accurately as follows. The data scatter in Figure 4 shows that  $k_4/k_{3a}$  is known to within  $\pm 15\%$  throughout this temperature range. The uncertainty in  $k_{3a}$  was estimated previously to be plus or minus a factor of 2, and this will dominate the error in  $k_4$  over the measured temperature range. Thus,  $k_4$  (297–404 K) can be represented by the following expression to within a factor of 2.

$$\begin{aligned} k_4 &= k_{3a}(k_4/k_{3a}) = 1.6 \times 10^{-11} k_4/k_{3a} \\ &= 1.6 \times 10^{-11} \times 10^{23.56} e^{-(12700)/RT} \\ &= 5.8 \times 10^{12} e^{-(12700)/RT} \text{ s}^{-1} \end{aligned} \quad (\text{C})$$

Results from this experimental expression for  $k_4$  can be compared to the rate constants calculated from ab initio expressions derived in five determinations of the rate constant for decarboxylation reaction 9, which is a reaction very similar to reaction 4, at temperatures from 297 to 404 K.



The recommended rate constant expressions from these five ab initio calculations and the rate constants calculated from them at 297 and 400 K are presented in Table 4. The most complete published ab initio calculation of  $k_9$  is that of Tan et al.,<sup>6</sup> who calculated not only the temperature dependence but also the effect of pressure on  $k_9$ . As shown in Table 4,  $k_9$  from this reference is predicted to be near its high-pressure limit at ambient temperature and 1 atm total pressure, although the predicted rate rises 20% at 10 atm and then falls off slightly as the pressure increases further at ambient temperature. At 400 K, the predicted rate constant increases monotonically with pressure until the high pressure limit is reached at a factor of  $\sim 3$  times that at 1 atm. Zhao et al.<sup>23</sup> presents an ab initio calculation for  $k_9$  at several pressures up to and including 10 atm. Farooq et al.<sup>3</sup> derived an expression for  $k_9$  by ab initio calculation and tested it using shock tube measurements of  $\text{CO}_2$  generation from the thermal decomposition of three methyl esters over the temperature range 1260 to 1653 K and 1.4 to 1.7 atm in the shock tube. The pressure used in the ab initio calculation is not stated by Farooq et al. Glaude et al.<sup>24</sup> performed an ab initio calculation of  $k_9$  for use in modeling atmospheric-pressure dimethyl carbonate flames. No pressure was stated for this ab initio calculation. In an unpublished

private communication, Klippenstein<sup>25</sup> also calculated  $k_9$  as a function of temperature and pressure. Although Klippenstein did not present a high-pressure limiting rate constant, stopping instead at 100 atm, his results show a monotonic approach to 100 atm at both 297 and 400 K rather than the nonmonotonic results of Tan et al. at 297 K. Finally, the ab initio potential energy surface was also derived for  $k_9$  by McCunn et al.<sup>4</sup> These authors did not derive a rate constant. They did identify the cis configuration of the methoxy carbonyl radical as by far the more favorable transition state for reaction 9, and the calculated energy above initial reactants of that transition state is 14.6 kcal  $\text{mol}^{-1}$  (see Figure 18 of that reference).

The experimental Arrhenius rate constant measured herein for  $k_4$  and the five ab initio calculations of the non-Arrhenius rate constant expression for  $k_9$  are compared in Table 4 over the temperature range 297 to 400 K. I believe that it is reasonable to assume that the decarboxylation of the two carbonyl radicals should have similar rate constants and transition state energies based on their structural similarity. Table 4 also presents the Arrhenius expressions derived from the non-Arrhenius ab initio rate constants over the temperature range 297–404 K. This provides a clearer comparison of the rate constants from the ab initio calculations with the measured rate constant expression for the ethoxy carbonyl radical. The rate constant  $k_4$  will be closer to its high pressure limit than is  $k_9$  at 1 atm throughout the measured temperature range because it has significantly more vibrational degrees of freedom. For this reason, I believe that the best comparison of the calculated rate constants to this experiment can be obtained using the high pressure limiting rate constants from the ab initio calculations where available. Klippenstein<sup>25</sup> presents a value for  $k_9$  at 100 atm, which must be at or very near the high pressure limit within this temperature range as confirmed by the pressure-dependent calculations of  $k_9$  and  $k_{9\infty}$  by Tan et al.<sup>6</sup> which are presented in Table 4.

Figure 6 presents the rate constant curves generated by the five ab initio calculations of the decarboxylation of the methoxy carbonyl radical for comparison to the curve (red line) measured in the current experiments for the ethoxy carbonyl radical. The factor of 2 uncertainty estimated for the experimental measurement of the decarboxylation of the ethoxy carbonyl radical is indicated by the red vertical line. The experimental result, while for a different but very similar radical, provides the only data against which to compare the gas phase ab initio calculations of the decarboxylation of the methoxy carbonyl radical to my knowledge. All of the curves are linear over the experimental temperature range. The 100 atm line of Klippenstein's calculation of  $k_9$  (line 2, blue) lies on the experimental line for the ethoxy carbonyl radical. The  $k_{9\infty}$  line of Tan et al. (line 3, black) lies close to the experimental line, nearly within the estimated factor of 2 error in  $k_4$ . These two ab initio calculations are the best choices for comparing to  $k_4$ , since both were derived at essentially the high-pressure limit. The calculations of Glaude et al. (line 4, green) and Farooq et al. (line 5, brown) are in reasonable agreement with  $k_4$  in light of the fact that the experimental results were obtained for a different albeit very similar alkoxy carbonyl radical and the pressures used for these two calculations are unstated. The ab initio rate constant of Zhao et al.<sup>23</sup> is derived from their 10 atm result. Based on the calculations of Tan et al. and Klippenstein, the Zhao et al. rate constant is at its high pressure limit at 297 K but in the falloff region at 400 K, resulting in an apparent value of  $E_a$ , which will be too low. Once again, however, this rate

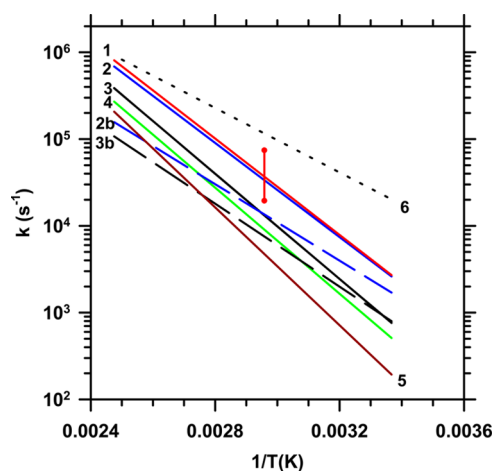


**Figure 6.** Plots of  $k_4$  and  $k_9$  vs  $1/T$ . Line 1 (red) =  $k_4$  from this work (see Table 4); vertical red line indicates estimated error of a factor of 2 as described in the text. 2 (blue) = ab initio calculation of  $k_9$  at 100 atm (ref 25). 2b (dashed blue) = ab initio calculation of  $k_9$  at 1 atm (ref 25). 3 (black) = ab initio calculation of  $k_{9,\infty}$  (ref 6). 3b (dashed black) = ab initio calculation of  $k_9$  at 1 atm (ref 6). 4 (green) = ab initio calculation of  $k_9$  at an unstated pressure (ref 24). 5 (brown) = ab initio calculation of  $k_9$  at an unstated pressure (ref 3). 6 (black dotted) = ab initio calculation of  $k_9$  at 10 atm (ref 23).

constant is in decent agreement with the experimental data for  $k_4$  in the 297–404 K range.

The ethoxy carbonyl radical has a measured activation energy of  $12560 \pm 875 \text{ cal mol}^{-1}$  as described earlier in this section over the temperature range 297–404 K, in which the error limit includes the data scatter in  $k_4/k_{3a}$  and the error estimated for  $E_{a_{3a}}$ . This value can be compared to the activation energies of the Arrhenius expressions derived over the same temperature range for reaction 9 from the ab initio non-Arrhenius expressions presented in Table 4. Because reactions 4 and 9 might be expected to have similar activation energies, this comparison can provide a test of the ab initio calculations of  $E_{a_9}$  over this temperature range. Unfortunately, the effect of pressure on the rate constant ratio  $k_4/k_{3a}$  was not measured during these experiments because the laboratory space was taken out of service during a building renovation. However, as mentioned earlier,  $k_4$  must be closer to its high-pressure limit than  $k_9$  is throughout this temperature range because of the larger number of vibrational modes in the ethoxy carbonyl radical. The pressure dependent ab initio calculations of  $k_9$  predict that  $k_9$  is at its high pressure limit at 1 atm and 297 K, and only a factor of 3 below it at 1 atm and 400 K. It seems reasonable to assume that  $k_4$  will be very near to its high-pressure limit from 297 to 400 K at the experimental pressure of  $\sim 1$  atm. Thus, it is appropriate to compare the Arrhenius activation energy of  $k_4$  to the ab initio high-pressure Arrhenius activation energy values in Table 4 which were determined by Klippenstein<sup>25</sup> ( $12410 \text{ cal mol}^{-1}$ ) and by Tan et al.<sup>6</sup> ( $13880 \text{ cal mol}^{-1}$ ) for  $k_9$ .  $E_{a_4}$  agrees with the high-pressure values of  $E_{a_9}$  calculated by both of these authors to nearly within the experimental error estimated for  $E_{a_4}$ . As expected, as the pressure is lowered, the ab initio apparent activation energy of  $k_9$  decreases (see curves 2b and 3b in Figure 6) because, as the temperature increases,  $k_9$  at 400 K falls off to a greater extent than at 297 K. The value of  $E_{a_9}$  calculated by Zhao et al.<sup>23</sup> is the smallest of all the ab initio determinations as seen in Table 4 and Figure 6. Some of this difference can be attributed to the

fact that their calculations were performed at a maximum pressure of 10 atm. This is below the high pressure limit at 404 K as seen from the results of Klippenstein and of Tan et al. in Table 4, and will result in a reduced apparent activation energy. However, the value of  $E_{a_9}$  determined by Zhao et al. is considerably lower than that determined by Klippenstein<sup>25</sup> and by Tan et al.<sup>6</sup> at 10 atm as shown in Table 4.

#### 4.0. SUMMARY

Results from three separate kinetic and mechanistic studies on ethyl formate and the ethoxy carbonyl radical formed from ethyl formate are reported herein. The measurements are summarized below:

- (1) The ratio of the rate constant for reaction of ethyl formate with atomic chlorine (reaction 1) was measured relative to that of ethyl chloride with atomic chlorine (reaction 2) at 297 K and 1 atm, yielding  $k_1/k_2 = 1.09 \pm 0.05$ . This agrees with two previous measurements of this rate constant ratio to within the combined error limits.<sup>1,2</sup> Reaction 1 represents the sum of the hydrogen abstraction reactions from the three possible hydrogen atom sites in ethyl formate to form the free radicals  $\text{CH}_3\text{CH}_2\text{OC}(=\text{O})$  [reaction 1a],  $\text{CH}_3\text{CHOC}(=\text{O})\text{H}$  [reaction 1b], and  $\text{CH}_2\text{CH}_2\text{OC}(=\text{O})\text{H}$  [reaction 1c]. This experiment was carried out in mixtures of ethyl formate,  $\text{Cl}_2$ , and  $\text{N}_2$  using UV light to dissociate  $\text{Cl}_2$  into Cl atoms.
- (2) The yields of the three product radicals formed after H atom abstraction by Cl from ethyl formate were determined by measuring the yields of the stable chlorinated products  $\text{CH}_3\text{CH}_2\text{O}(\text{C}=\text{O})\text{Cl}$ ,  $\text{CH}_3\text{CHClO}(\text{C}=\text{O})\text{H}$ , and  $\text{CH}_2\text{ClCH}_2\text{O}(\text{C}=\text{O})\text{H}$ . These species are generated by the quantitative reactions of the free radical products with  $\text{Cl}_2$  in the initial mixture. The product radical yields from channels 1a, 1b, and 1c are  $25 \pm 3\%$ ,  $67 \pm 5\%$ , and  $8 \pm 2\%$ , respectively at 297 K. There is a small decrease in the product yield from channel 1b and a small increase in the product yield from channel 1c with increasing temperature. The product yield from reaction 1a remains constant to within experimental error over the temperature range 297 to 434 K. These experimental yields are compared with a recent ab initio calculation of the free radical yields from reaction 1.<sup>1</sup>
- (3) Finally, the rate constant for decarboxylation of the ethoxy carbonyl radical [ $\text{CH}_3\text{CH}_2\text{OC}(=\text{O}) \rightarrow \text{CH}_3\text{CH}_2 + \text{CO}_2$ , reaction 4] was measured relative to the rate constant of its reaction with  $\text{Cl}_2$  [ $\text{CH}_3\text{CH}_2\text{OC}(=\text{O}) + \text{Cl}_2 \rightarrow \text{CH}_3\text{CH}_2\text{OC}(=\text{O})\text{Cl} + \text{Cl}$ , reaction 3a] over the temperature range 297 to 404 K. The rate constant ratio determined at  $\sim 1$  atm can be expressed as  $k_4/k_{3a} = 10^{23.56 \pm 0.22} e^{-(12700 \pm 375)/RT} \text{ molecules cm}^{-3}$  in which the error limits are  $2\sigma$  but correlated. By estimating the value of  $k_{3a}$ , which has not been measured, based on similar reactions, the expression  $k_4 = 5.8 \times 10^{12} e^{-(12700)/RT} \text{ s}^{-1}$  is obtained. This expression has an estimated error of  $\pm$  a factor of 2 over the stated temperature range. These results are compared to recent ab initio calculations of the rate constant of the decarboxylation of methoxy carbonyl [ $\text{CH}_3\text{OC}(=\text{O})$ ], which is very similar structurally to the ethoxy carbonyl radical.

## AUTHOR INFORMATION

## Corresponding Author

\*E-mail: ewkaiser@comcast.net; Mailing address: 7 Windham Lane, Dearborn, MI 48120, United States.

## Notes

The authors declare no competing financial interest.

## ACKNOWLEDGMENTS

I thank Prof. Craig J. Donahue (University of Michigan-Dearborn) for his assistance during this research. I also thank Dr. William Pitz and Dr. Charles Westbrook of Lawrence Livermore National Laboratory for helpful discussions during the preparation of this manuscript.

## REFERENCES

- (1) Balaganesh, M.; Dash, M. R.; Rajakumar, B. Experimental and Computational Investigation on the Gas Phase Reaction of Ethyl Formate with Cl Atoms. *J. Phys. Chem. A* **2014**, *118*, 5272–5278.
- (2) Wallington, T. J.; Hurley, M. D.; Haryanto, A. Kinetics of the Gas-Phase Reactions of Chlorine Atoms with a Series of Formates. *Chem. Phys. Lett.* **2006**, *432*, 57–61.
- (3) Farooq, A.; Davidson, D. F.; Hanson, R. K.; Huynh, L. K.; Violi, A. An Experimental and Computational Study of Methyl Ester Decomposition Pathways using Shock Tubes. *Proc. Combust. Inst.* **2009**, *32*, 247–253.
- (4) McCunn, L. R.; Lau, K.-C.; Krisch, M. J.; Butler, L. J.; Tsung, J.-W.; Lin, J. J. Unimolecular Dissociation of the  $\text{CH}_3\text{OCO}$  Radical: An Intermediate in the  $\text{CH}_3\text{O} + \text{CO}$  Reaction. *J. Phys. Chem. A* **2006**, *110*, 1625–1634.
- (5) Bell, M. J.; Lau, K.-C.; Krisch, M. J.; Bennett, D. I. G.; Butler, L. J.; Weinhold, F. Characterization of the Methoxy Carbonyl Radical Formed via Photolysis of Methyl Chloroformate at 193.3 nm. *J. Phys. Chem. A* **2007**, *111*, 1762–1770.
- (6) Tan, T.; Yang, X.; Ju, Y.; Carter, E. A. Ab Initio Reaction Kinetics of  $\text{CH}_3\text{OC}(=\text{O})$  and  $\text{CH}_2\text{OC}(=\text{O})\text{H}$  Radicals. *J. Phys. Chem. B* **2016**, *120*, 1590–1600.
- (7) Simakov, P. A.; Martinez, F. N.; Horner, J. H.; Newcomb, M. Absolute Rate Constants for Alkoxy-carbonyl Radical Reactions. *J. Org. Chem.* **1998**, *63*, 1226–1232.
- (8) Beckwith, L. J. A.; Bowry, V. W. Kinetics of Reactions of Cyclopropylcarbonyl Radicals and Alkoxy-carbonyl Radicals Containing Stabilizing Substituents: Implications for Their Use as Radical Clocks. *J. Am. Chem. Soc.* **1994**, *116*, 2710–2716.
- (9) Bucher, G.; Halupka, M.; Kolano, C.; Schade, O.; Sander, W. Characterization of Alkoxy-carbonyl Radicals by Step-Scan Time-Resolved Infrared Spectroscopy. *Eur. J. Org. Chem.* **2001**, *2001*, 545–552.
- (10) Kaiser, E. W.; Wallington, T. J.; Hurley, M. D. Products and Mechanism of the Reaction of Cl with Butanone in  $\text{N}_2/\text{O}_2$  Diluent at 297–526 K. *J. Phys. Chem. A* **2009**, *113*, 2424–2437.
- (11) Kaiser, E. W.; Pierce, D. S. Study of the Thermodynamics (Thermal and Cl Catalyzed) and Kinetics of the Cis and Trans Isomerizations of  $\text{CF}_3\text{CF}=\text{CHF}$ ,  $\text{CF}_3\text{CH}=\text{CHCF}_3$ , and  $\text{CH}_3\text{CH}=\text{CHCH}_3$  in 100–950 Torr of  $\text{N}_2$  Diluent at 296–875 K: Effect of F and  $\text{CF}_3$  Substitution on the Isomerization Process Including the Fluorine “Cis Effect”. *J. Phys. Chem. A* **2015**, *119*, 9000–9017.
- (12) Braun, W.; Herron, J. T.; Kahaner, D. K. Acuchem: A Computer Program for Modeling Complex Chemical Reaction Systems. *Int. J. Chem. Kinet.* **1988**, *20*, 51–62.
- (13) Taatjes, C. A.; Christensen, L. K.; Hurley, M. D.; Wallington, T. J. Absolute and Site-Specific Abstraction Rate Coefficients for Reactions of Cl with  $\text{CH}_3\text{CH}_2\text{OH}$ ,  $\text{CH}_3\text{CD}_2\text{OH}$ , and  $\text{CD}_3\text{CH}_2\text{OH}$  between 295 and 600 K. *J. Phys. Chem. A* **1999**, *103*, 9805–9814.
- (14) Wallington, T. J.; Hurley, M. D.; Maurer, T.; Barnes, I.; Becker, K. H.; Tyndall, G. S.; Orlando, J. J.; Pimentel, A. S.; Bilde, M. Atmospheric Oxidation Mechanism of Methyl Formate. *J. Phys. Chem. A* **2001**, *105*, 5146–5154.
- (15) Malanca, F. E.; Fraire, J. C.; Arguello, G. A. Kinetics and Reaction Mechanism in the oxidation of Ethyl Formate in the Presence of  $\text{NO}_2$ : Atmospheric Implications. *J. Photochem. Photobiol., A* **2009**, *204*, 75–81.
- (16) Saito, K.; Oda, A.; Tokinaga, K. High Temperature Unimolecular Decomposition of Ethyl Chloroformate: Comparison of the Secondary Competing Steps with Ethyl Formate. In *Shock Waves @ Marseille II: Physico-Chemical Processes and Nonequilibrium Flow*, Proceedings of the 19th International Symposium on Shock Waves Held at Marseille, France, 26–30 July 1993; Brun, R., Dumitrescu, L. Z., Eds.; Springer: New York, 1995; pp. 119–124.
- (17) Maricq, M. M.; Szente, J. J. The UV Spectrum of Acetyl and the Kinetics of the Chain Reaction between Acetaldehyde and Chlorine. *Chem. Phys. Lett.* **1996**, *253*, 333–339.
- (18) Gierczak, T.; Rajakumar, B.; Flad, J. E.; Burkholder, J. B. Rate Coefficients for the Reaction of the Acetyl Radical,  $\text{CH}_3\text{CO}$ , with  $\text{Cl}_2$  between 253 and 384 K. *Int. J. Chem. Kinet.* **2009**, *41*, 543–553.
- (19) Timonen, R. S.; Ratajczak, E.; Gutman, D. Kinetics of the Reactions of the Formyl Radical with Oxygen, Nitrogen dioxide, Chlorine, and Bromine. *J. Phys. Chem.* **1988**, *92*, 651–655.
- (20) Ninomiya, Y.; Goto, M.; Hashimoto, S.; Kagawa, Y.; Yoshizawa, K.; Kawasaki, M.; Wallington, T. J.; Hurley, M. D. Cavity Ring-Down Spectroscopy and Relative Rate Study of Reactions of HCO Radicals with  $\text{O}_2$ ,  $\text{NO}$ ,  $\text{NO}_2$ , and  $\text{Cl}_2$  at 295 K. *J. Phys. Chem. A* **2000**, *104*, 7556–7564.
- (21) Maricq, M. M.; Szente, J. J.; Hybl, J. D. Kinetic Studies of the Oxidation of Dimethyl Ether and its Chain Reaction with  $\text{Cl}_2$ . *J. Phys. Chem. A* **1997**, *101*, 5155–5167.
- (22) Timonen, R. S.; Gutman, D. Kinetics of the Reactions of Methyl, Ethyl, Isopropyl, and Tert-butyl Radicals with Molecular Chlorine. *J. Phys. Chem.* **1986**, *90*, 2987–2981.
- (23) Zhao, L.; Xie, M.; Ye, L.; Cheng, Z.; Cai, J.; Li, Y.; Qi, F.; Zhang, L. Corrigendum to “An Experimental and Modeling Study of Methyl Propanoate Pyrolysis at Low Pressure.”. *Combust. Flame* **2013**, *160*, 1958–1966.
- (24) Glaude, P. A.; Pitz, W. J.; Thomson, M. J. Chemical Kinetic Modeling of Dimethyl Carbonate in an Opposed Flow Diffusion Flame. *Proc. Combust. Inst.* **2005**, *30*, 1111–1118.
- (25) Klippenstein, S. J., private communication included in the data compilation [http://www.nuigalway.ie/c3/documents/56.53\\_release.chem](http://www.nuigalway.ie/c3/documents/56.53_release.chem).